Int. J. Pres. Ves. & Piping **27** (1987) 367–384

An Elastic–Plastic Analysis of the Integral Tubesheet in U-tube Heat Exchangers—Towards an ASME Code Oriented Approach

A. I. Soler
Vice President, Holtec International

and

K. P. Singh
President, Holtec International

(Received 4 October 1986; accepted 30 October 1986)

ABSTRACT

The tubesheet in a U-tube heat exchanger with integral shell and channel joints may develop high discontinuity stresses at these joints. Evaluation of the structural support provided by the shell and the channel to the tubesheet must consider the possibility of plastic hinges at the shell/tubesheet and channel/tubesheet joints. An incremental elastic–plastic analysis is herein presented which treats the formation of the plastic hinge in a systematic and conservative manner. A practical, somewhat more conservative, design procedure is also proposed for possible inclusion in the ASME Code, Section VIII Div. I rules.

NOMENCLATURE

a	radius of perforated region
b	outer radius of unperforated region of tubesheet
D	generic term for flexural rigidity of a plate or shell type structure
e	flexural efficiency
E^*, ν^*	effective elastic constants of tubesheet perforated region

Int. J. Pres. Ves. & Piping 0308-0161/87/$03·50

E	Young's moduli of tubesheet
h	tubesheet thickness
K_a	rotational spring rate of the outer edge of the perforated region
M^*	edge loading parameter
M_0	radial bending moment at $r = a$ (per unit circumference)
M_r, M_θ	radial, circumferential bending moments in perforated region of tubesheet
M_R	effective ring moment
M_c, M_s	channel, shell edge bending moments
p	differential pressure across tubesheet
p_c, p_s	tubeside, shellside pressure, respectively
t_c, t_s	channel, shell thickness
δ^*	increase in shell/channel radius due to membrane effect of pressure
δ, θ	edge deflection, rotation of shell, channel
μ	edge stiffness parameter
σ_y	specified stress limit (eqn (18))
ε	plasticity parameter

Subscripts

c	pertains to the channel (tubeside)
R	pertains to the tubesheet rim
s	pertains to the shell

INTRODUCTION

U-tube heat exchangers with the tubesheet integrally welded to the shell and to the channel are quite common in the power and process industries. Typically, the thicknesses of the shell and the channel in such an exchanger are calculated using the appropriate code rules (viz. ASME Boiler and Pressure Vessel Code in the U.S. and many other countries). The thickness of the tubesheet is usually computed from the formulas given in the TEMA Standards.[1] The TEMA tubesheet thickness formula, essentially based on the works of the late Karl Gardner, takes the restraining effect of the welded channel and shell into account in an approximate manner. The local membrane and bending stresses developed at the shell/tubesheet, and channel/tubesheet junction, are neither calculated nor are they required to be limited, which is consistent with Section VIII Div. I of the ASME Code. However, in applications involving high pressures in the channel or the shell side, a complete stress analysis of a TEMA designed unit frequently shows the local stresses to be greater than the material yield point, indicating some permanent deformation at the joint, and consequent loss of some of the restraining influence from the yielded member (channel or shell). Stress analysis oriented versions of the ASME Boiler and Pressure Codes, such as Section VIII Div. 2, recognize the dichotomous status of discontinuity stresses between a shell and flat structure. They postulate that the combined bending and membrane stress at the junction must be less than the material yield strength (stated as 1·5 times the nominal allowable stress) if the contribution of the shell member to reducing the plate member's bending stress is to be included in the analysis. Design oriented codes, on the other hand, such as Section VIII Div. I, restrict their rules to limiting primary stresses only. The ASME Code has recently published a thickness computation method for gasketed tubesheets in a non-mandatory appendix.[2] In the next step, presumably, the formulas will be extended to the integral tubesheet construction—the topic of this paper. At this stage, the Code must wrestle with the issue of the contribution of the welded shell and/or channel. An obvious answer to the question is to disregard the restraining effect. Besides being ostensibly conservative, this also possesses the virtue of simplicity—an essential attribute to merit inclusion in the Code. However, such an approach would produce tubesheet thicknesses as much as 20% greater than the time-proven TEMA formula results, especially in high-pressure applications. This approach is also *unconservative* in many cases when applied to integral *fixed* tubesheet constructions. As pointed out in Ref. 3 (Chapter 9), tubesheets designed with a simply supported edge condition assumption may, in some practical cases, actually be overstressed in the presence of a restraining shell or channel! While such anomalies do not afflict an unstayed tubesheet construction, such as a U-tube unit, considerations of economy warrant additional thought into ways to incorporate the edge restraining effects of welded in shell and/or channel. Moreover, the designer should have the latitude to 'thicken' the adjoining shell member (shell or channel) instead of adding to the tubesheet thickness. In fact, in high-pressure applications, the tubesheets are frequently forged with an integral channel stub. It is relatively economical to add to the thickness of the channel stub, and is usually preferable to increasing the tubesheet thickness, since the latter entails increased tube hole drilling, reaming and (sometimes) the tube expansion costs.

The above considerations prompted us to develop a solution procedure to treat the integrally welded U-tubesheet problem assuming the shell and channel material to be elastic—perfectly plastic. This solution is a direct extension of the elastic analysis presented in Chapter 8 of Ref. 3, and therefore draws heavily on the formulation detailed herein.

In this paper we investigate whether it is feasible, in a routine design environment, to evolve a simple enough procedure which permits credit for adjacent barrel strengthening of the tubesheet only up to the point when the barrel/tubesheet junction forms a plastic hinge, and then removing the interaction of the barrel for any loading subsequent to this point. What we are proposing, of course, is to examine the viability of a design procedure which applies the loading in stages and permits formation of 'yield hinges' in the barrel when specified stress limits are achieved. Such a design procedure can, of course, be achieved numerically using any one of a number of commercially available Finite Element Codes. The Finite Element Codes are not, however, adaptable to design code procedures. Therefore, we propose to consider herein the question of applying the incremental analysis to a formulated set of analytical design equations. For simplicity, we illustrate our proposal using a high-pressure U-tube unit as a design case; we recognize, however, that it is in fixed tubesheet exchangers with integral tubesheets where these new considerations may offer the best return on the investment of additional complexities in the design procedure.

Having carried out the elastic–plastic analysis, we suggest a further simplification to the solution procedure which may render this treatment suitable for use in a design code.

ANALYSIS

We begin with a summary of the relevant design equations for U-tube heat exchanger tubesheets found in Ref. 3. In particular, we focus attention on two sided integral construction. Referring to Fig. 1 (reproduced from Ref. 3), the equations for maximum stresses in the tubesheet, in the channel barrel, and in the shell barrel, have the form

$$\sigma_{TS} = 6M_{\max}/h^2 \tag{1}$$

where $M_{\max}$= the magnitude of the maximum radial bending moment in the tubesheet (either at $r=0$ or $r=a$).

$$\sigma_c = \frac{p_c b}{2t_c} + \frac{6}{t_c^2}|M_c| \tag{2}$$

$$\sigma_s = \frac{p_s b}{2t_s} + \frac{6}{t_s^2}|M_s| \tag{3}$$

For the moment, we let $\dot{M}$, $\dot{V}$, $\dot{\delta}$ and $\dot{\theta}$ represent incremental changes in either shell or channel bending moment, shear force, radial displacement, and cross-sectional rotation. Positive directions for these quantities are

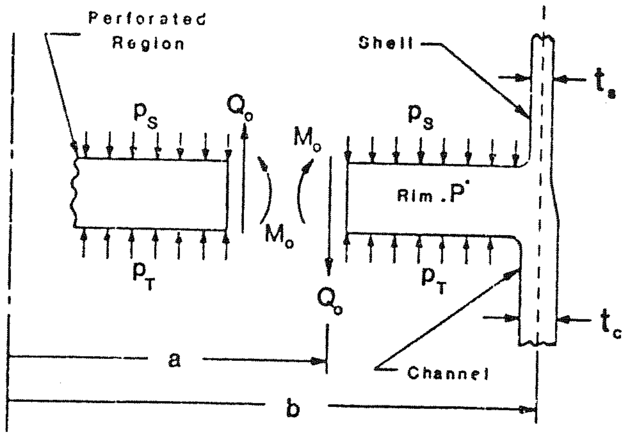

Fig. 1. Two-side integral construction.

shown in Fig. 2. If radial stretch of the tubesheet is disregarded, then compatibility demands that

$$\dot{\delta}_c = \frac{h}{2}\dot{\theta}_R; \qquad \dot{\delta}_s = -\frac{h}{2}\dot{\theta}_R \tag{4}$$

where θ_R is the rotation of the tubesheet ring.

For either shell or channel we may write the elastic constitutive equations in the forms

$$\dot{\delta} = \frac{\alpha_{11}\dot{V}b^3}{D} - \alpha_{12}\frac{\dot{M}b^2}{D} - \dot{\delta}^* \tag{5}$$

$$\dot{\theta} = -\frac{\alpha_{12}\dot{V}b^2}{D} + \alpha_{22}\frac{\dot{M}b}{D} \tag{6}$$

In eqns (5) and (6), b is the mean radius of the shell or head, $D = Et^3/12(1 - \nu^2)$, δ^* is the outward radial movement of a free shell under internal pressure, and α_{ij} are the functions of t/b given below:

$$\begin{aligned} \alpha_{11} &= 0{\cdot}235\,64(t/b)^{1{\cdot}5} \\ \alpha_{12} &= 0{\cdot}302\,89t/b \\ \alpha_{22} &= 0{\cdot}778\,68(t/b)^{0{\cdot}5} \end{aligned} \tag{7}$$

Using eqn (5) in eqn (4) yields a solution for V in terms of M, δ and θ_R for both the shell and channel. For subsequent use, we form the relation

$$\dot{M} + \frac{h}{2}\dot{V} = \dot{\psi}$$

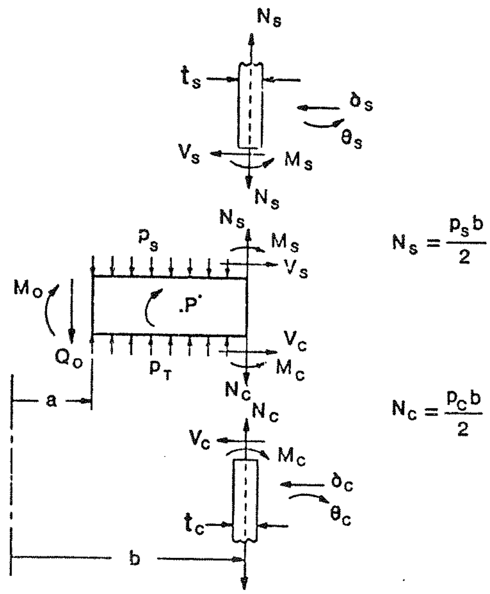

Fig. 2. Free body analysis of two-sided integral construction.

and obtain, after elimination of $\dot{V}$,

$$\dot{\psi} = \frac{\dot{M}}{\alpha_{11}}\left(\alpha_{11} + \alpha_{12}\frac{h}{2b}\right) + \frac{h}{2b}\frac{\dot{\delta}^* D}{\alpha_{11} b^2} \pm \frac{h^2}{4b^2}\frac{D\dot{\theta}_R}{\alpha_{11} b} \tag{8}$$

Equation (8), valid for either the shell or head, has been derived without use of eqn (6) and therefore is valid regardless of whether we consider the joint to be elastic or to have yielded.

To eliminate $\dot{M}$ from eqn (8) requires that a choice of elastic or plastic action at the joint be established. If the reaction is elastic during an increment, then eqn (6) provides a mechanism for eliminating $\dot{M}$ from eqn (8). If the joint has yielded, then in any subsequent load increment, we assume that a relation between $\dot{M}$ and $\dot{N}$ (the axial load resultant increment) exists in the form

$$\dot{M} + \alpha\dot{N} = 0 \tag{9}$$

If we insist that the extreme fiber stress undergoes no change, then, from eqns (2) or (3), $\alpha = t/6$. If, instead, we assume a linear relation between M/My and N/Ny (where My, Ny are the moment and force on a fully yielded section) during cross section yielding, then $\alpha = My/Ny = t/4$. For our subsequent analysis, we use $\alpha = t/4$ since this gives a faster reduction of the cross-sectional bending moments after the onset of cross-sectional plastic rotation. Let us consider the final form for eqn (8) when the structure is elastic during the increment. Solving for $\dot{M}$ from eqn (6) yields

$$\dot{M}b = \pm\frac{\dot{\theta}_R D}{K^*} + \frac{\alpha_{12}\dot{\delta}^* D}{bJK^*} \tag{10}$$

where K^*, J have the form (for either shell or head)

$$K^* = \frac{\alpha_{11}\alpha_{22} - \alpha_{12}^2}{\alpha_{11} + \alpha_{12}\dfrac{h}{2b}}; \qquad J = \alpha_{11} + \alpha_{12}\frac{h}{2b} \tag{11}$$

We now introduce a parameter ε, which has the value unity when the joint is elastic during an increment, and the value zero when the section has yielded; then for either the elastic or yielded case, the moment increment can be written as

$$\dot{M} = -\frac{t\dot{N}}{4}(1-\varepsilon) + \varepsilon\left[\frac{\alpha_{12}D}{b^2JK^*}\dot{\delta} \pm \frac{\dot{\theta}_R D}{K^* b}\right] \tag{12}$$

Eliminating $\dot{M}$ from eqn (8) by using eqn (12) yields the general expression for $\dot{\psi}$ (for either shell or channel) as

$$b\dot{\psi} = \left(\dot{M} + \frac{h}{2}\dot{V}\right)b = -\frac{J}{\alpha_{11}}(1-\varepsilon)b\frac{t\dot{N}}{4}$$
$$\pm\,\dot{\theta}_R\frac{D}{K^*\alpha_{11}}\left[\varepsilon J + \frac{h^2}{4b^2}K^*\right] + \frac{D\dot{\delta}^*}{\alpha_{11}b}\left[\varepsilon\frac{\alpha_{12}}{K^*} + \frac{h}{2b}\right] \tag{13}$$

Let us consider Fig. 2 which shows a free body of the ring under incremental forces and moments from the tubesheet, shell and channel. Using eqn (13) and introducing subscripts s and c for the shell and head increment tending to rotate the ring yields

$$\dot{\theta}_R D_R \ln\frac{b}{a} = a\dot{M}_0 + \frac{\Delta\dot{p}}{4}a^3(K^2+1)(K-1) + b\left[\dot{M}_s + \frac{h}{2}\dot{V}_s - \dot{M}_c - \frac{h}{2}\dot{V}_c\right] \tag{14}$$

Using eqn (13) and introducing subscripts s and c for the shell and head respectively, yields a final incremental equation relating θ_R, M_0, and the incremental pressures p_c, p_s. We write this equation in the form

$$a\dot{M}_0 = D^*(1+\nu)\mu\dot{\theta}_R + a\dot{M}^* \tag{15}$$

where $D^* = E^*h^3/12(1-\nu^{*2})$ and E^*, ν^* are the effective elastic constants for the perforated region of the tubesheet. The expressions for μ and $\dot{M}^*$ allowing for yielding at either or both shell and head connection to tubesheet can be written as:

$$\mu D^*(1+\nu^*) = D\left[\ln\frac{b}{a}+\lambda\right] \tag{16}$$

$$\lambda = \frac{D_c}{DK_c^*\alpha_{11}^c}\left[\varepsilon_c J_c + \frac{h^2}{4b^2}K_c^*\right] + \frac{D_s}{DK_s^*\alpha_{11}^s}\left[\varepsilon_s J_s + \frac{h^2}{4b^2}K_s^*\right]$$

$$\dot{M}^* = -\frac{\Delta\dot{p}a^2}{4}(K^2+1)(K-1) + \frac{J_s}{\alpha_{11}^s}\frac{K(1-\varepsilon_s)}{8}\dot{p}_s\frac{b^2 t_s}{a} - \frac{J_c K}{\alpha_{11}^c}(1-\varepsilon_c)\frac{b^2 t_c}{a}\dot{p}_c$$

$$-\frac{D_s}{\alpha_{11}^s}\frac{\dot{\delta}_s^*}{ba}\left(\varepsilon_s\frac{\alpha_{12}^s}{K_s^*}+\frac{h}{2b}\right) + \frac{D_c}{\alpha_{11}^c}\frac{\dot{\delta}^*}{ab}\left(\varepsilon_c\frac{\alpha_{12}^c}{K_c^*}+\frac{h}{2b}\right) \tag{17}$$

We note that eqns (16) and (17) reduce to the forms given in Ref. 3 (eqns (8.3.12) to (8.3.14)), when the joint rotation occurs entirely in the elastic regime.

Once μ and $\dot{M}^*$ are determined for the general loading increment, it is a straightforward matter to compute the important stress increments in the tubesheet, head and shell region.

ELASTIC–PLASTIC ANALYSIS PROCEDURE

We suggest the following incremental design analysis procedure.

Step 1

Assume the unit remains elastic in the tubesheet, head and shell through the entire load range; apply the total load in a single increment and calculate the critical design stresses in tubesheet, head and shell, accounting for all interactions between tubesheet, head and shell. If none of the prescribed stress limits are exceeded, the design is acceptable, or a series of refined analyses may be undertaken to remove metal from understressed regions. If the tubesheet is overstressed, repeat the analysis with new geometry until the stress levels are acceptable. If either (or both) head or shell critical stresses are too high, while the tubesheet is understressed, then proceed to Step 2. (For subsequent discussion, we assume that the joint stress in the channel reaches its design limit first.)

Step 2

Find the critical applied load increment such that the critical joint stress in the head just reaches its code-designated limiting value. Calculate all stress increments corresponding to this load increment.

Step 3

Set the plasticity parameter $\varepsilon_c = 0$ for subsequent loading and determine whether the next load increment is sufficient to reach the maximum load state or will cause yielding at the shell joint.

Step 4

If the tubesheet is understressed, the sum of the initial load increments is still below the maximum load to be applied, the tubesheet stress is still within limits, but the shell has now reached yield, then set the parameter $\varepsilon_s = 0$, apply a final load increment and check whether the tubesheet stress level remains below the critical value.

Use of the above design procedure will permit the user to take selective credit for rotational restraint provided by the shell and channel: that is, rotational restraint to the tubesheet will only be present while the shell and head stresses remain below the specified design limit.

COMPUTER IMPLEMENTATION

The above design procedure is conceptually simple and offers the possibility of significant material savings in certain configurations; however, because of the significant increase in computational requirements to check a particular geometry, the design procedure suggests computer implementation. In this paper, we examine the potential application of the microcomputer code TK! Solver[4] to the U-tube incremental design procedure. This general purpose equation solver does not require the user to make a permanent choice of dependent variables: that is, desired unknowns can be on either side of the 'equal sign' in an equation; at the beginning of the solution phase, the user specifies what the problem unknowns are by his choice of input data. The TK! Solver code either solves the equations directly or automatically applies an iterative solution scheme. While the code may require significant solution time if the equations are highly non-linear, the designer need not become involved in any significant programming effort. The formulation of a TK! Solver simulation requires the user only to input the governing equations using BASIC. Reference 5 provides the necessary information concerning application of TK! Solver to a multitude of simulations.

Table 1 shows the complete 'rule sheet' for the U-tube incremental design procedure, while Table 2 shows the 'variable sheet' together with a typed-in set of input data and the results obtained. In Table 2 we have neglected

TABLE 1
Design Rules

S Rule

```
st = 6 * max(abs(ma), abs(m0))/(h * h)/1e
ma = (ms + 0·125 * mu * (pc − ps) * a * a)/(1 + mu)
m0 = ma − (3 + nu) * (pc − ps) * a * a/16
rr = a * (ma − ms)/(e * (1 + nu) * mu) * (10·92/(et * h^3))
sc = pc * b/tc + abs(6 * mh/(tc * tc)) + 0/e1 + 0/(tc − 0·000000 1)
mh = −(1 − e1) * pc * tc/8 + e1 * (ec * tc^3/10·92)/b * (3·301 4 * b/tc * (dc/b) + rr * kc) + 0/(tc − 0·000
dc = pc * b * b/(2 * ec * tc) * 1·7
kc = 2·568 * (b/tc)^0·5 + 1·651 * (h/tc)
ss = ps * b/ts + abs(6 * mb/(ts * ts)) + 0/e2 + 0/(ts − 0·000000 1)
mb = −(1 − e2) * ps * ts/8 + e2 * (es * ts^3/10·92)/b * (3·301 4 * b/ts * (ds/b) − rr * ks) + 0/(ts − 0·000
ds = ps * b * b/(2 * es * ts) * 1·7
ks = 2·568 * (b/ts)^0·5 + 1·651 * (h/ts)
mu = (1/(e * (1 + nu))) * (ln(b/a) + z1 + z2)
z1 = ec/et * (tc/h)^3 * kc/(0·23564 * (tc/b)^1·5) * (e1 * jc + (h/(2 * b))^2/kc)
z2 = es/et * (ts/h)^3 * ks/(0·23564 * (ts/b)^1·5) * (e2 * js + (h/(2 * b))^2/ks)
jc = (0·23564 * (tc/b)^1·5) * (1 + 0·642696 5 * h/((b * tc)^0·5))
js = (0·23564 * (ts/b)^1·5) * (1 + 0·642696 5 * h/((b * ts)^0·5))
ms = −0·25 * (pc − ps) * a * a * ((b/a)^2 + 1) * (b/a − 1) + x1 + x2 + x3 + x4
x1 = (1 + 0·6426965 * h/((b * ts)^0·5)) * (1 − e2) * b/a * ps * b * ts/8
x2 = −(1 + 0·6426965 * h/((b * tc)^0·5)) * (1 − e1) * b/a * pc * b * tc/8
x3 = −(es * ts^3/10·92) * ds/(b * a * (0·23564 * (ts/b)^1·5)) * (e2 * 0·302 89 * ts/b * ks + h/(2 * b))
x4 = +(ec * tc^3/10·92) * dc/(b*a*(0·23564*(tc/b)^1·5)) * (e1 * 0·302 89 * tc/b * kc + h/(2 * b))
```

edge support from either the shell or the channel and determined what tubesheet thickness h is required to support a tubeside pressure of 2000 psi. The shell and head interaction is removed by assuming the Young's modulus and thickness of the head and shell to be very small. Table 2 shows that a tubesheet thickness $h = 13{\cdot}29$ in is required to support a tubesheet having an outer radius = 26 in and a perforated radius = 24 in. The maximum tubesheet stress in this application is 26 250 psi and is an input quantity in Table 2.

Table 3 shows the output from the TK! Solver solution if full interaction between tubesheet, head, and shell is accounted for in a unit with a 3 in thick channel and a 1 in thick shell. The tubesheet geometry is as shown in Table 2 and the material is steel. The pressure loading of 2000 psi is applied in a single step and the tubesheet maximum bending stress is required to reach 26 250 psi. We see that the tubesheet thickness needed is 9·15 in; however, the channel bending stress at the tubesheet-head joint is 61 484 psi which is well above $1{\cdot}5S_a$ (material yield point). We see that the full effect of including shell-head rotational resistance translates, in this case, to a 4 in reduction in required tubesheet thickness albeit at the expense of overstressing the channel.

TABLE 2
Typical Variable Sheet

St Input	*Name*	*Output Unit*	*Comment*
			ANALYSIS NEGLECTING EDGE SUPPORT
26 250	st		max tubesheet bending stress
	sc		max stress in channel
	ss		max stress in shell barrel
2 000	pc		tubeside pressure (INPUT?)
0	ps		shellside pressure (INPUT?)
	ma	−22429·73	moment at r = a
	m0	−262189·7	moment at r = 0·0
	mh		max moment in head
	mb		bending moment in shell
	ms	−52151·33	moment parameter M*
	mu	0·17858347	rotational stiffness parameter
	z1	3·416E-20	channel rotation contribution
	z2	3·416E-20	shell rotation contribution
	rr	0·00143083	rotation of unperforated rim
	dc	1·1492E13	displacement of head due to pressure
	ds	0	displacement of shell due to pressure
1	e1		plasticity factor for head (INPUT)
1	e2		shell plasticity factor (INPUT)
	h	13·286143	thickness of tubesheet (INPUT)
26	b		outer radius of assembly (INPUT)
24	a		radius of perforated region (INPUT)
0·3395	le		ligament efficiency (INPUT)
0·33	nu		effective Poisson's Ratio (INPUT)
0·3369992	e		ratio of D/D* (INPUT)
29000000	et		Young's Modulus of tubesheet (INPUT)
1	ec		Young's Modulus of head (INPUT)
1	es		Young's Modulus of shell (INPUT)
0·0000001	tc		thickness of channel (INPUT)
0·0000001	ts		thickness of shell (INPUT)
	kc	219395627	parameter (1/K*) for head
	jc	2·977E-10	parameter J for head
	ks	219395627	parameter (1/K*) for shell
	js	2·977E-10	parameter J for shell
	x1	0	parameter in MSTAR equation
	x2	0	parameter in MSTAR equation
	x3	0	parameter in MSTAR equation
	x4	15·335466	parameter in MSTAR equation

TABLE 3
TK! Solver Output—Full Interaction

St Input	*Name*	*Output Unit*	*Comment*
			FULL SUPPORT NO PLASTICITY
26250	st		max tubesheet bending stress
	sc	61484·265	max stress in channel
	ss	13004·820	max stress in shell barrel
2000	pc		tubeside pressure (INPUT?)
0	ps		shellside pressure (INPUT?)
	ma	115413·32	moment at r = a
	m0	−124346·7	moment at r = 0·0
	mh	66226·398	max moment in head
	mb	−2167·470	bending moment in shell
	ms	49095·421	moment parameter M*
	mu	2·3198884	rotational stiffness parameter
	z1	0·85773809	channel rotation contribution
	z2	0·10201390	shell rotation contribution
	rr	7·5248E-4	rotation of unperforated rim
	dc	0·01320920	displacement of head due to pressure
	ds	0	displacement of shell due to pressure
1	e1		plasticity factor for head (INPUT)
1	e2		shell plasticity factor (INPUT)
	h	9·1497278	thickness of tubesheet (INPUT)
26	b		outer radius of assembly (INPUT)
24	a		radius of perforated region (INPUT)
0·339 5	le		ligament efficiency (INPUT)
0·33	nu		effective Poisson's Ratio (INPUT)
0·336 999 2	e		ratio of D/D* (INPUT)
29 000 000	et		Young's Modulus of tubesheet (INPUT)
29 000 000	ec		Young's Modulus of head (INPUT)
29 000 000	es		Young's Modulus of shell (INPUT)
3	tc		thickness of channel (INPUT)
1	ts		thickness of shell (INPUT)
	kc	12·595388	parameter (1/K*) for head
	jc	0·01538519	parameter J for head
	ks	28·200483	parameter (1/K*) for shell
	js	0·00382724	parameter J for shell
	x1	0	parameter in MSTAR equation
	x2	0	parameter in MSTAR equation
	x3	0	parameter in MSTAR equation
	x4	101262·09	parameter in MSTAR equation

TABLE 4
TK! Solver Output—First Pass

St Input	Name	Output Unit	Comment
			RUN 3-LIMIT SC TO 26 250 AND FIND PC
	st	9957·9518	max tubesheet bending stress
26250	sc		max stress in channel
	ss	4928·5817	max stress in shell barrel
	pc	895·41733	tubeside pressure (INPUT?)
0	ps		shellside pressure (INPUT?)
	ma	50997·219	moment at r = a
	m0	−56345·41	moment at r = 0·0
	mh	27734·575	max moment in head
	mb	−821·4303	bending moment in shell
	ms	24836·864	moment parameter M*
	mu	1·9751127	rotational stiffness parameter
	z1	0·71749524	channel rotation contribution
	z2	0·08772521	shell rotation contribution
	rr	2·7165E-4	rotation of unperforated rim
	dc	0·00591387	displacement of head due to pressure
	ds	0	displacement of shell due to pressure
1	e1		plasticity factor for head (INPUT)
1	e2		shell plasticity factor (INPUT)
10	h		thickness of tubesheet (INPUT)
26	b		outer radius of assembly (INPUT)
24	a		radius of perforated region (INPUT)
0·3395	le		ligament efficiency (INPUT)
0·33	nu		effective Poisson's Ratio (INPUT)
0·3369992	e		ratio of D/D* (INPUT)
29000000	et		Young's Modulus of tubesheet (INPUT)
29000000	ec		Young's Modulus of head (INPUT)
29000000	es		Young's Modulus of shell (INPUT)
3	tc		thickness of channel (INPUT)
1	ts		thickness of shell (INPUT)
	kc	13·063321	parameter (1/K*) for head
	jc	0·01595665	parameter J for head
	ks	29·604282	parameter (1/K*) for shell
	js	0·00401773	parameter J for shell
	x1	0	parameter in MSTAR equation
	x2	0	parameter in MSTAR equation
	x3	0	parameter in MSTAR equation
	x4	47742·332	parameter in MSTAR equation

TABLE 5
TK! Solver Output—Last Pass

St Input	*Name*	*Output Unit*	*Comment*
			RUN 4 PLASTIC HINGE CHAN.
	st	21494·436	max tubesheet bending stress
0	sc		max stress in channel
	ss	25144·487	max stress in shell barrel
1104·5827	pc		tubeside pressure (INPUT?)
0	ps		shellside pressure (INPUT?)
	ma	10794·687	moment at r = a
	m0	−121622·7	moment at r = 0·0
	mh	−414·2185	max moment in head
	mb	−4190·748	bending moment in shell
	ms	−31513·46	moment parameter M*
	mu	0·61552315	rotational stiffness parameter
	z1	0·10811506	channel rotation contribution
	z2	0·08772521	shell rotation contribution
	rr	0·00138591	rotation of unperforated rim
	dc	0·00729532	displacement of head due to pressure
	ds	0	displacement of shell due to pressure
0	e1		plasticity factor for head (INPUT)
1	e2		shell plasticity factor (INPUT)
10	h		thickness of tubesheet (INPUT)
26	b		outer radius of assembly (INPUT)
24	a		radius of perforated region (INPUT)
0·3395	le		ligament efficiency (INPUT)
0·33	nu		effective Poisson's Ratio (INPUT)
0·3369992	e		ratio of D/D* (INPUT)
29000000	et		Young's Modulus of tubesheet (INPUT)
29000000	ec		Young's Modulus of head (INPUT)
29000000	es		Young's Modulus of shell (INPUT)
3	tc		thickness of channel (INPUT)
1	ts		thickness of shell (INPUT)
	kc	13·063321	parameter (1/K*) for head
	jc	0·01595665	parameter J for head
	ks	29·604282	parameter (1/K*) for shell
	js	0·00401773	parameter J for shell
	x1	0	parameter in MSTAR equation
	x2	−20157·47	parameter in MSTAR equation
	x3	0	parameter in MSTAR equation
	x4	17455·203	parameter in MSTAR equation

With the above limiting results in hand, we turn now to an application of the incremental design technique. We assume that it is desired to hold the head and shell thicknesses at 3 in and 1 in, respectively, and our goal is simply to determine the tubesheet thickness, h (where $9{\cdot}15\,\text{in} < h < 13{\cdot}29\,\text{in}$), consistent with accounting for head and shell rotational resistance only while the respective component bending stress is below the prescribed limit. Table 4 shows the results of a first elastic pass where we assume $h = 10\,\text{in}$, limit the head bending stress extreme fiber value to 26 250 psi, and determine the value of the tubeside pressure increment. We see that $\Delta p = 895$ psi results in a tubesheet bending stress increment $\Delta\sigma_{TS} = 9958$ psi and a shell bending stress increment $\Delta\sigma_s = 4929$ psi. Recall that we have forced the head bending stress $\Delta\sigma_s = 26\,250$ psi. Table 5 shows the result of the subsequent pressure increment $\Delta p = 1105$ psi (so as to reach a maximum tubeside pressure = 2000 psi after the two increments. We see that the assumed thickness h is not viable since both the tubesheet and shell stress increments in the second pass are such to cause the total tubesheet and shell stress to exceed the prescribed limits.

The foregoing steps are repeated with the assumed tubesheet thickness as 11·0 in. We find that the head limiting stress is reached at tubeside pressure = 940 psi and gives a tubesheet bending stress increment of $\Delta\sigma_{TS} = 8708$ psi. The subsequent increment (with no rotational resistance credited to the head) applied a tubeside pressure change of $(2000 - 940 = 1060\,\text{psi})$ and yields $\Delta\sigma_{TS} = 17\,278$ psi. Thus, for this 11 in tubesheet, no credit is taken for rotational resistance of the head after a tubeside pressure of 940 psi is applied, and the final tubesheet bending stress is $17\,278 + 8708 = 25\,986$ psi. We see that for this particular configuration, the new incremental design procedure effects a 2 in thick change in tube sheet thickness from the purely elastic design and ensures that ASME Code concepts are met.

A NON-ITERATIVE DESIGN PROCEDURE

The foregoing elastic–plastic analysis is quite attractive as a computer-aided design tool. However, it is too complicated to be suitable for inclusion in the design codes. It is possible to devise a non-iterative, straightforward design procedure which gives tubesheet thickness which lies between the elastic–plastic solution and the simply supported edge solution. The method can be outlined in the following four steps:

(1) For a given tubesheet thickness, compute the edge rotation θ_R^* assuming simply supported support at $r = b$.

(2) Compute the shell edge bending stress σ_s, and channel edge bending stress σ_c corresponding to this edge rotation θ_R^*.
(3) If both σ_c and σ_s are below their respective permitted stress limits, then no further calculation is necessary. If the computed σ_c or σ_s exceed the specified limit, then modify the corresponding Young's modulus proportionately, i.e.

$$E_c' = E_c \frac{\sigma_y^c}{\sigma_c}$$
$$E_s' = E_s \frac{\sigma_y^s}{\sigma_s} \quad (18)$$

In the above, σ_y represents the specified stress limit.
(4) Re-compute the tubesheet bending stress corresponding to the modified (as necessary) shell and channel Young's moduli.

The above procedure is based on the concept that the edge rotation under simply supported end conditions θ_R^* would be an upper bound on the true edge rotation of the tubesheet. Therefore, the shell and channel edge moments corresponding to θ_R^* are upper bounds on the actual value.

Modifying the Young's moduli in the above manner has the effect of keeping the edge restraint moment below the limit moment for all values of $\theta_R < \theta_R^*$. Since the solution point value of θ_R is guaranteed to be below θ_R^*, a lower bound assessment of edge restraint is assured.

The required set of equations are extracted from Ref. 3 below to illustrate the solution procedure.

The rotation θ_R of the tubesheet outer ring is related to the moment factor M^* and stiffness parameter μ by the relation

$$\theta_R = \frac{\left(\frac{pa^3}{8} - aM^*\right)}{(1+\mu)D_R e(1+\nu^*)} \quad (19)$$

where

$$\mu = \frac{\lambda_2 + \ln\frac{b}{a}}{e(1+\nu^*)} \quad (20)$$

$$M^* = -\frac{pa^2}{4}\left(\frac{b^2}{a^2}+1\right)\left(\frac{b}{a}-1\right) \quad (21)$$

$$\lambda_2 = \frac{D_s}{D_R K_s^*}\left[1 + \frac{hK_{0s}}{2b}\right] + \frac{D_c}{D_R K_c^*}\left[1 + \frac{hK_{0c}}{2b}\right] \quad (22)$$

K_s^* and K_c^* are given by eqn (11), and can be further simplified as

$$K^* = \left[2{\cdot}568\left(\frac{b}{t}\right)^{1/2} + 1{\cdot}651\left(\frac{h}{t}\right)\right]^{-1} \tag{23}$$

$$K_0 = 3{\cdot}301K^*\frac{b}{t}\left[1 + 1{\cdot}285\left(\frac{h^2}{bt}\right)^{1/2}\right] \tag{24}$$

with proper subscripts, (c or s) appended to K^*, K_0 and t.

Finally, the edge moments are given by

$$\begin{aligned} M_c &= \frac{D_c}{bK_c^*}\theta_R + 0{\cdot}2572p_ct_cb \\ M_s &= \frac{D_s}{bK_s^*}\theta_R + 0{\cdot}2572p_st_sb \end{aligned} \tag{25}$$

Setting $\lambda_2 = 0$ in eqn (20) gives μ for the simply supported edge condition, say μ^*. μ^*, substituted for μ in eqn (19) gives θ_R^*, which in turn gives M_c^* and M_s^* from eqn (25) for the purely elastic solution. Substituting for M_c and M_s in eqns (2) and (3) gives the corresponding shell and channel stresses.

The elastic moduli are then modified according to eqn (18); and the corrected λ_2 (eqn (22)), μ (eqn (20)) and θ_R (eqn (19)) are computed.

The maximum tubesheet bending stress follows from eqn (1), where

$$M_{\max} = \text{largest of } [M_r(a), M_\theta(a), M_r(0)]$$

$$\begin{aligned} M_r(a) &= \frac{M^*}{1+\mu} + \frac{\mu}{1+\mu}\frac{pa^2}{8} && \text{(a)} \\ M_\theta(a) &= \frac{M^*}{1+\mu} - \frac{pa^2}{8}\left(1 - v^* - \frac{\mu}{1+\mu}\right) && \text{(b)} \\ M_r(0) &= \frac{M^*}{1+\mu} - \frac{pa^2}{16}\left(3 + v^* - \frac{2\mu}{1+\mu}\right) && \text{(c)} \end{aligned} \tag{26}$$

CONCLUSION

The state of stress in the tubesheet under lateral pressure, including the elastic–plastic restraining effect of the integral shell and channel, has been studied. The formation of plastic hinge, at the tubesheet/shell and tubesheet/channel junction and subsequent stress field changes, are computed using an incremental procedure. Incorporation of the edge restraints is found to reduce the required tubesheet thickness considerably in the example problem. The incremental solution technique requires use of a computer. A non-incremental solution technique, amenable to hand calculation, is therefore presented which gives consistently conservative results compared to the incremental solution. The latter method is offered as a possible candidate for use in the ASME Code.

REFERENCES

1. *Standards of Tubular Exchanger Manufacturer's Association*, sixth edn, TEMA, Inc., Tarrytown, New York, 1978.
2. Boiler and Pressure Vessel Code, Section VIII Div. I, ASME, New York, 1983.
3. Singh, K. P. and Soler, A. I., *Mechanical design of heat exchangers and pressure vessel components*, Arcturus Publishers, Cherry Hill, New Jersey, 1984.
4. TK! Solver, Software Arts, Inc., 1982.
5. Konapasek, M. and Jayaraman, S., *TK! Solver book*, Osborne-McGraw Hill, Berkeley, California, 1984